




# Asymmetric Fission Transmission of Linear-to-Circular Polarization Converter Using Bi-layer Split Ring Structure

Farman Ali Mangi<sup>1</sup>  · Shaoqiu Xiao<sup>2</sup> · Qasim Ali Arain<sup>3</sup>  ·  
Imran Memon<sup>4</sup>  · Ghulam Fatima Kakepoto<sup>2</sup>

Published online: 28 December 2017

© Springer Science+Business Media, LLC, part of Springer Nature 2017

**Abstract** A circular polarizer based on bi-layer split ring structure is proposed that could achieve asymmetric fission transmission of linearly polarized wave at the dual band. Firstly, a new approach of “Fission Transmission of Electromagnetic (FTEM) waves” is introduced to understand the polarization transformation behavior for linear-to-circular polarization. The designed structure achieves broadband circularly polarized wave with an asymmetric transmission over resonance frequencies by the principle of FTEM wave. The electronics circuit of proposed structure demonstrates the transformation behavior of EM waves when the electric and magnetic coupling between the upper and lower patterned SRR is reached at the certain strength. The physics of the giant circular dichroism effect and optical activity is illustrated by the surface currents distribution on the structure. The proposed structure achieves a right-handed circularly polarized wave and left hand circularly polarized wave with high transmission at 13.94–15.70 GHz and at 16.0–17.03 GHz, respectively. The axial ratio bandwidth of 11.76 and 6.86% is obtained at the dual band. The simulated and measured results exhibit good correspondence.

**Keywords** Axial ratio (AR) · Circular polarization · Fission transmission · Chain transmission and split ring resonator

---

✉ Farman Ali Mangi  
farman.mangi@salu.edu.pk

<sup>1</sup> Department of Physics and Electronics, Shah Abdul Latif University Khairpur, Khairpur, Sindh, Pakistan

<sup>2</sup> School of Physical Electronics, University of Electronic Science and Technology of China, Chengdu 610054, Sichuan, People’s Republic of China

<sup>3</sup> Beijing University of Posts and Telecommunications (BUPT), Beijing, People’s Republic of China

<sup>4</sup> College of Computer Science, Zhejiang University, Hangzhou 310027, Zhejiang People’s Republic of China

## 1 Introduction

Polarization control of electromagnetic waves has long been a concern for the wide range of applications in modern satellite and communication system. The circular polarizer is a basic device in antennas with circular polarization because it manipulates the polarization state and obtains the phase difference  $90^\circ$  between two decomposed orthogonal linear components [1]. The circular polarization has better performance to offer the superior transmission signal over the linearly polarized wave. Many transmission type circular polarizers are introduced, such as grating structure, U-shape split ring resonators, metallic helices, meandered lines and parallel plates [2–10]. Furthermore, various configurations are presented for constructing dual-band circular polarizers, such as structure based on twisted Q-shaped metasurface [11], split ring resonator [12–14], thin dual-band polarizer was introduced for satellite applications [15]. The multi-band circular polarizer based on periodic metallic strip array [16]. Though, all introduced structures are affected by the bandwidth limitation over the operating frequencies.

Widening bandwidth is an important issue in polarizer research. However, lots of polarizers, such as the metamaterial polarizer, usually operate over narrow band. The circular dichroism was obtained across a narrow band at resonance frequencies [17]. The broadband polarizer limits the use of narrow band polarizers in high gain multi-beam antenna systems. Therefore, the transmission-type circular polarizers are more attractive to avoid the band limitation due to the cut-off characteristic of waveguide circular polarizer [18]. The wider bandwidth of SRR can be achieved by using different values of loaded capacitor and inductor in equivalent RLC circuit [19].

The polarization rotating FSS which is based on SIW cavity resonator was introduced to enhance the bandwidth from 4.6 to 7.2% [20]. The circular polarizer constructed of single layer of split ring resonator achieved bandwidth of 8% at resonant frequencies [21]. Recently, a new structure was proposed to realize circular polarization at 35 GHz and achieved bandwidth of 9.1% [22].

In this paper, asymmetric fission transmission of linear-to-circular polarization converter using bi-layer split-ring structure is introduced which is based on the principle of FTEM wave. The analogy to the structure in [23], the SRRs array pattern is adopted with different dimensions on the both sides of the substrate to achieve more resonance frequencies when electric field impinges on the designed structure along the x-direction.

Firstly, the innovative approach of FTEM wave is presented, which transforms linearly polarized (giant optical activity) wave into the circular polarized (strong circular dichroism) wave. It means that the x-polarized wave impinges on the proposed polarizer along the + z direction, the two orthogonal linearly polarized components can emerge through the bottom layer. The two transformed components from bottom-layer are used as excitation source for upper-layer. Finally, the four orthogonal linear components emerge at the end of structure and converted in circular polarization. This impinging and transmission sequence of the orthogonal components constitutes the chain transmission of the linearly polarized wave. We present the mechanism of asymmetric transmission which is attributed to designed structure. The proposed structure achieves RHCP wave and LHCP wave with high transmission at 13.94–15.70 and 16.0–17.03 GHz, respectively.

The high transmission efficiency and axial ratio bandwidth at dual-band are the good advantages of proposed design which are relatively better than reported work. The designed structure is simple and can be easily fabricated. The increasing number of unit cell printed on both sides of the dielectric substrate is subjected to enhance the axial ratio

bandwidth at resonance frequencies. Meanwhile, the proposed structure is also suitable to design the application of microwave devices and scaled into higher frequencies ranges.

## 2 Design Principle and Theoretical Analysis

Figure 1 a, b represent the layout of the unit cell and two-dimensional array of asymmetric fission transmission of linear-to-circular polarization converter. The two types of split ring resonator of the perfect electric conductor (PEC) with different dimensions are patterned on each side of substrate Roger. The period constant is denoted by parameter  $p$  and the thickness of substrate denoted by  $t$ . The width is both patterned SRR assumed to be  $w$  while the outer and inner radii of both identical rings are denoted by  $r_1$  and  $r_2$ .  $D$  is shown the opening rings (whereas,  $D_1$  and  $D_2$  are the horizontal opening space of upper and bottom SRR). The thickness of SRR layers on both sides of the substrate is represented by  $t_m$ . The

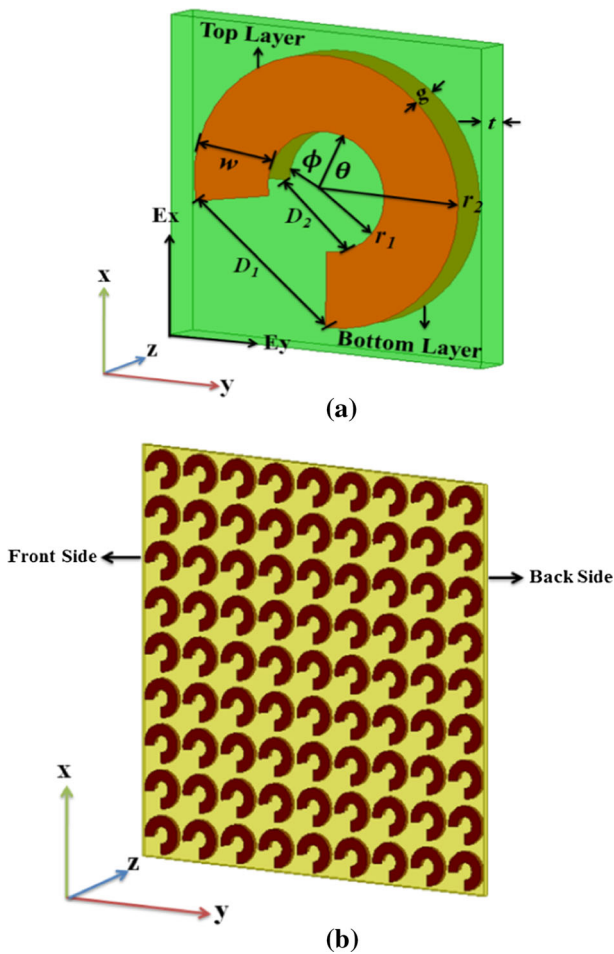


**Fig. 1** a Perspective of the unit cell, b asymmetric fission transmission of linear-to-circular polarization converter

central angle of each ring is identically represented by  $\theta$ . The printed rings of the back side of the substrate are twisted by an angle of  $\phi$  with respect to the printed ring on the front side.

The dielectric Roger RT/duroid5880 is selected with relative permittivity as  $\epsilon_r = 2.2$  with loss tangent of 0.0009. The following geometry dimensions parameters are follows as  $p = 8$  mm,  $t = 0.787$  mm,  $w = 1.87$  mm,  $r_1 = 1.5$  mm,  $r_2 = 3.4$  mm,  $D_1 = 2.8$  mm,  $D_2 = 3.4$  mm,  $t_m = 0.01$  mm  $\theta = 280^\circ$ ,  $\phi = 270^\circ$ .

The designed structure is fabricated into  $9 \times 9$  unit cells sample. The array occupies an overall area of  $72$  mm  $\times$   $72$  mm. Figure 2 shows the photograph of sample of structure. The experiment is performed through free space in microwave anechoic chamber.

The transmission characteristics of the proposed structure are analyzed by using ANSYS HFSS. The periodic boundary conditions are set to the x- and y-directions. The linearly polarized wave is applied along the + z direction to excite the structure. The constructed structure has the strong strength to achieve giant CD effect due to strong coupling between the electric and magnetic field. The fabricated sample is tested by performing the experiment.

In the measurement, the sample and distance between the pair of horn antennas are adjusted to ensure the far field zone. The sample is perpendicularly placed in middle position between two linearly polarized horn antennas. The standard antennas are connected to vector network analyzer Agilent N5230C to measure the co-and cross-transmission characteristics of the sample. The vector components of the EM wave can be obtained by changing the orientation of antennas. The receiver antenna is rotated from horizontal to the vertical direction to measure the cross-polar transmission. The measured co-polarization reference is utilized for the cross-polar measurements. The raw data is shown in oscillating behavior; therefore, a data processing procedure similar as in Ref. [24] is used to remove oscillations behavior from data.

The phenomenon of polarization conversion is defined by using electric circuit of designed structure depicted in Fig. 3. The bi-layer of SRR is introduced in this structure to obtain equivalent orthogonal linearly polarized waves at the end of the upper layer with  $90^\circ$  phase difference for the incident of x- linear polarization. However, the twisted SRR at the both sides of the structure have enough potential to convert linear-to-circular

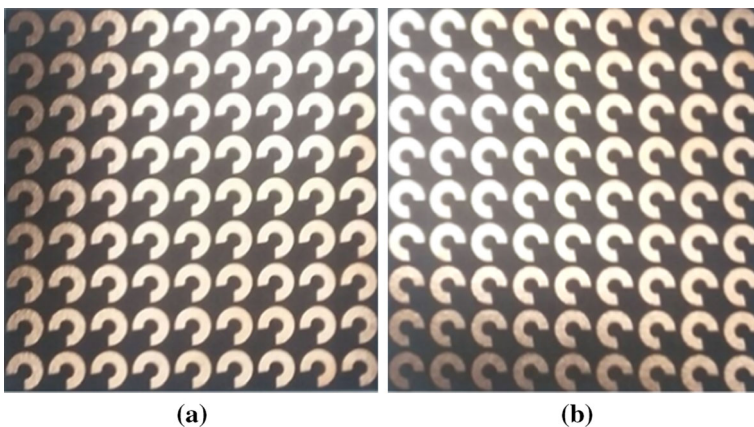


**Fig. 2** The photograph of fabricated sample **a** represents the top view and **b** shows the bottom view of the designed structure

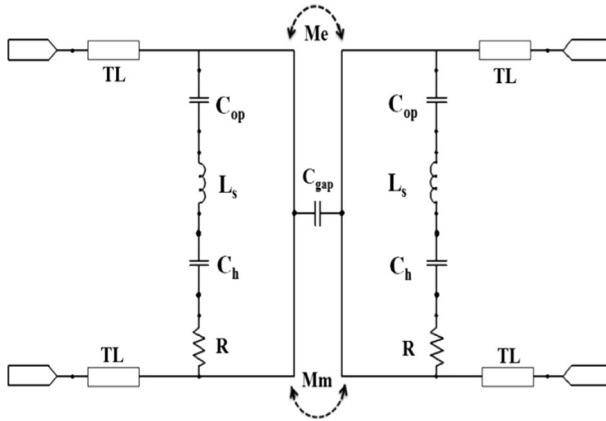


**Fig. 3** Depicts the equivalent RLC circuit of structure

polarization due to the magnetic and electric field mutual coupling between them. The proposed structure based on bi-layer of SRR modeled by an equivalent electric circuit which consists of inductor-capacitor series resonant circuits. The coupling resonance of proposed structure is described by the RLC resonant circuit.

The proposed structure is composed of the metal SRR due to array pattern adopted with different dimensions on the both sides of substrate. The horizontal opening space of the rings is modeled by capacity  $C_{op}$ . The each ring corresponds to the solenoid that is shown by inductance  $L_s$ . In addition, the overall capacity created between two horizontal SRR of the structure can be represented by  $C_h$ . The overall electric and magnetic interaction between upper and lower twisted SRR creates the mutual capacitance introduced by  $C_{gap}$ , respectively. The implemented metal SRR are adopted with inductance  $L_s \approx \mu_o(r_2 + w/2) \ln(2r_2/w + 1)$  and capacitance  $C_{op} \approx \epsilon_o t_m / 2D$ . The resonant frequency  $f_0$  can be determined based on the geometric parameter of DSRR. The printed SRRs consist of perfect electric conductor PEC with inductance “L” and a capacitance “C” attribute to opening space or gap between two SRR, respectively. The modeled electric circuit RLC series circuit with resonance frequency can be shown as follow. The resonant frequency ‘ $f_0$ ’ of upper and lower layers may be expressed based on geometric parameters of the structure.

$$f_0 = \frac{1}{2\pi\sqrt{L_s(C_{op} + C_h)}} \approx \frac{1}{2\pi\sqrt{LC}} \tag{1}$$

According to RLC series circuit, the L is the total inductance and C is the total capacitance of the structure. The capacitance  $C_{gap}$  created between two perpendicular patterned rings expressed as follow.

$$C_{gap} = \frac{\epsilon_r \epsilon_0 S}{g} \tag{2}$$

$$C_{gap} = \frac{\epsilon_r \epsilon_0 \left[ \left( \frac{\pi\phi}{360} \right) (r_2^2 - r_1^2) \right]}{g} \tag{3}$$

whereas the “S” represents the area between upper and lower SRR and  $S = \pi\phi/360 (r_2^2 - r_1^2)$ . The  $r_1$  and  $r_2$  show the outer and inner and outer radii of the lower SRR. The electric and magnetic coupling described by the Euler–Lagrange equation and the eigen-frequencies of coupled structure can be obtained by solving this equation.

$$f_{\pm} = f_o \cdot \frac{\sqrt{1 \pm K_e \cdot \left\{ \cos(\theta - \phi) - a[\cos(\theta - \phi)^2 + b[\cos(\theta - \phi)^3] \right\}}}{(1 \pm K_m)} \tag{4}$$

where  $K_e = M_e/L$  and  $K_m = M_m/L$  are represented by the coefficients of coupling of electric and magnetic between two layers of the structure, which is the functions of the angle between  $\theta$  and  $\phi$ ; whereas, a and b are expressed by numerical factors. The overall interaction of electric and magnetic are described by capacitance and mutual inductance of twisted DSRR in order to  $(\theta - \phi) = 10^\circ$ , respectively.

Based on the physics of coupling effect, the co-and cross- polarization transmission characteristics are considered for the case of twisted angle  $(\theta - \phi) = 10^\circ$ . The impinged electric field travel toward the polarizer in the + z direction.

The technique is applied to calculate the transmission characteristics of the designed structure are discussed. The incident linearly polarized wave travel toward the polarizer in the + z direction. The incident linearly polarized wave can be decomposed into two orthogonal vector linearly polarized components of equal magnitude with  $90^\circ$  phase difference between them. The two orthogonal components provide two linear phase responses with phase difference of  $90^\circ$  to realize circular polarization. The structure manipulates polarization transformation based on impedance matched for both co-and cross polarization transmission providing two linear phase difference of  $90^\circ$  response. Based on these principles, the designed structure offers wideband operation. The impinged wave can be expressed as

$$E_i = E_x = \hat{x}E_0e^{ik_zz}. \tag{5}$$

The transmitted electric field along + z direction is determined as

$$E_t = \hat{x}T_{xx}E_i + \hat{y}T_{xy}E_i \tag{6}$$

where  $T_{xx}$  and  $T_{xy}$  are the transmission coefficients of co- and cross- polarization. Assuming that  $T_{xx} = E_x^t/E_x^i$  and  $T_{xy} = T_{yx} = E_y^t/E_x^i$  show the transmittance of x-to-x and x-to-y polarization conversions. In fission transmission of EM wave, the impinged x-linearly polarized wave is converted into to two orthogonal components. Meanwhile, the two transformed components through bottom layer  $E_x^t$  and  $E_y^t$  are used as linearly incident polarized waves  $E_x^i$  and  $E_y^i$  for upper of the structure. The following equation is expressed for the incident and transmission along the + z direction from bottom layer of the structure.

$$\text{Bottom-Layer-1} \quad \begin{bmatrix} E_x^t \\ E_y^t \end{bmatrix} = \begin{bmatrix} t_{xx} \\ t_{yx} \end{bmatrix} [E_x^i]. \tag{7}$$

The two transformed waves impinge on the interface of the toplayer along + z direction and four linear waves can be obtained at the end structure. Meanwhile, the incident and transmission of the linearly polarized wave from the top-layer can be expressed as

$$\begin{aligned} \text{Top-Layer-2} \quad \begin{bmatrix} E_x^{t21} \\ E_y^{t21} \end{bmatrix} &= \begin{bmatrix} t_{xx} \\ t_{yx} \end{bmatrix} [E_x^{t1}] \\ \begin{bmatrix} E_x^{t22} \\ E_y^{t22} \end{bmatrix} &= \begin{bmatrix} t_{xy} \\ t_{yy} \end{bmatrix} [E_y^{t1}]. \end{aligned} \quad (8)$$

The sum of Eqs. (7) and (8)

$$\begin{bmatrix} E_x^{t2} \\ E_y^{t2} \end{bmatrix} = \begin{bmatrix} t_{xy} & t_{xy} \\ t_{yx} & t_{yy} \end{bmatrix} \begin{bmatrix} E_x^{t1} \\ E_y^{t1} \end{bmatrix}. \quad (9)$$

In the end of the structure, the strong CD effects can be obtained due to strong coupling between electric field and magnetic field. The approach of FTEM wave expatiates the physical behavior of linear-to-circular polarization conversion and strong coupling of an electric and magnetic field to achieve giant optical activity and strong CD effects.

### 3 Simulated and Experimental Results

In simulated and measured results, the co- and cross-polar coefficients are obtained 7.52(7.93) dB, 5.42(4.92) and 4.60(5.13) dB, 1.58(1.98) dB are achieved  $f_1 = 14.56$  GHz and  $f_2 = 16.98$  GHz as shown in Fig. 4a, b. The axial ratio  $20\log_{10}(|T_{xy}/T_{xx}|)$  and phase difference  $\varphi(|T_{xy}|) - \varphi(|T_{xx}|)$  are achieved along the +z direction. The phase difference is calculated to be  $90.13^\circ(91.64^\circ)$  and  $-285.95^\circ(-285.34^\circ)$  at  $f_1$  and  $f_2$ . The axial ratio between transmission is obtained 0.60 dB (0.65 dB) at  $f_1$  and 0.29 dB (0.40 dB) at  $f_2$ , as depicted in Fig. 4c, d. The large axial ratio bandwidths is obtained which is broader at 13.94–15.70 GHz, BW = 11.76% and 16.0–17.03 GHz, BW = 6.86% respectively. The proposed structure achieves RHCP wave and LHCP wave with high transmission at 13.94–15.70 GHz and at 16.0–17.03 GHz, respectively.

The simulated and measured results exhibit good correspondence that indicate the extracted values have the least difference and slight frequency shift between numerical and experimental curves. The high transformation efficiency is clearly demonstrated from lower to higher frequency ranges as depicted in Fig. 4a, b. The amplitudes of  $T_{xx}$  and  $T_{xy}$  are nearly same around resonance frequencies from 13.94 to 15.70 GHz and 16.0–17.03 GHz, respectively.

In this particularly designed structure, the CD effect and purely circular polarized wave are achieved for the x-linearly polarized wave. It is noticed that the co- and cross-polarization wave are highly transmitted from lower to the higher frequency range and converted into circular polarization wave.

The surface current distributions elucidate the polarization transformation behavior and interpret the asymmetric transmission at distinct resonant frequencies. The simulated surface current distributions are denoted in Fig. 5a–d which illustrate the resonance behavior of structure at 14.56 and 16.98 GHz. The mechanism of strong CD and optical activity can be determined by the coupling of the electric and magnetic field. Based on the current distribution between layers, the in-phase currents are attributed to electric response and the anti-phase lead to the magnetic response which generates the electromagnetic response between two layers. In Fig. 5a–d, the solid (dash) line arrows indicate the surface current distribution on the top and bottom layers at 14.56 and 16.98 GHz. The two current

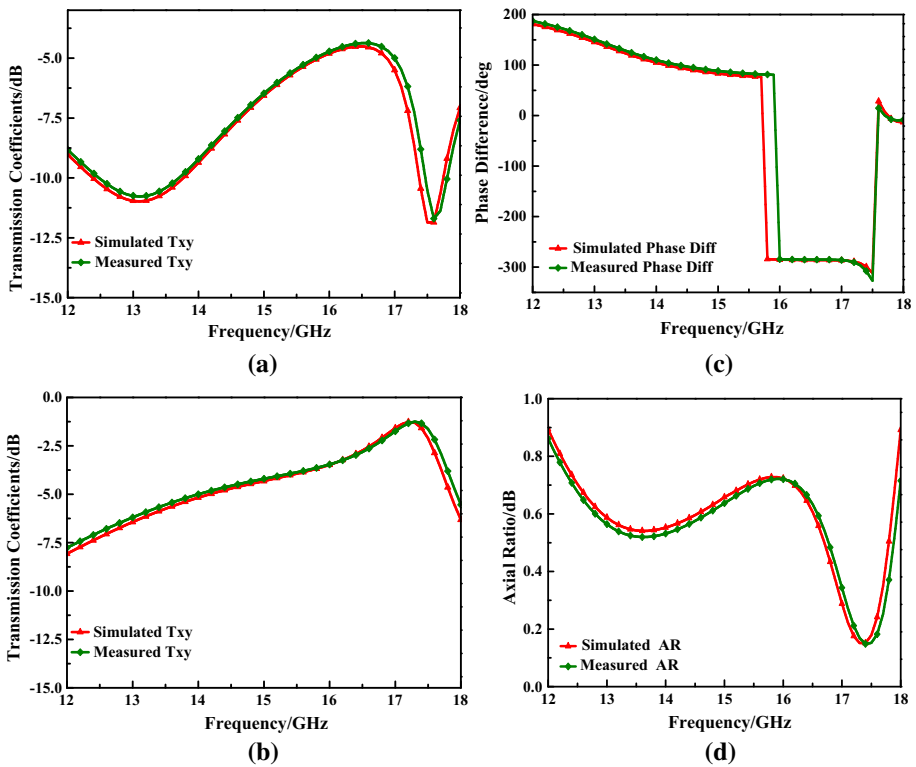


**Fig. 4** The simulated and measured results **a, b** transmission coefficients versus frequency, **c, d** phase difference versus frequency and axial the ratio between cross-co-polarization versus frequency

modes are distributed at the operating resonant frequency. One is dipole and other is loop mode which moves on the both sides of printed layers.

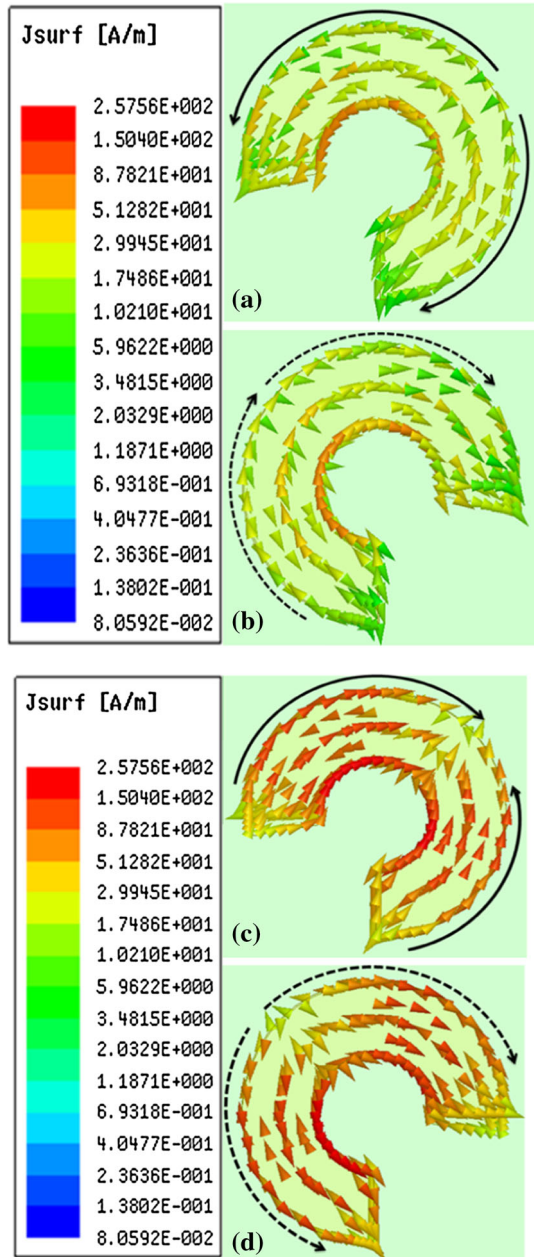
The surface currents occur in same directions on bottom metallic layer which attribute to symmetric resonance mode and the direction of surface currents on the top layer moves antiparallel which corresponds to an asymmetric resonance mode at lower frequency range as shown in Fig. 5a, b. In Fig. 5c, d, the strong coupling of electric and magnetic field enhancement occurs on top and bottom layers along x and y-direction at higher frequency range. It indicates that the giant circular dichroism effect results from the electric and magnetic dipole resonance.

The antiparallel surface currents direction on both sides of structure at higher frequencies which show the effective currents loops. The resonance frequencies of proposed structure can be changed by adjusting the electric circuit parameters of LC. The bandwidth can be controlled by adjusting the parameters length and opening gap  $D$  of SRR. In this discussion, the surface currents distributions on both sides of structure are antiparallel at higher frequency range which indicates the antiparallel magnetic dipole moment with asymmetric transmission wave.

Figure 5a, b represent the direction of surface currents on the top and bottom layers are not identical. Based on the observation, the antiphase surface currents distribution on the top and bottom layers realize the giant circular polarization conversion in the structure at 16.98 GHz as denoted in Fig. 5c, d, respectively.



**Fig. 5** **a, b** The simulated surface current distributions on top and bottom layers at  $f_1 = 14.56$ , and **c, d** the simulated surface current distributions on top and bottom layers at  $f_2 = 16.98$



The in-phase and anti-phase currents direction on the top and bottom layers at lower frequency and higher frequency ranges exhibit the characteristics of an electric and magnetic dipole. The in-phase currents determine the electric resonance and antiphase illustrate magnetic resonance response [25–28]. In addition, the electric and magnetic response exists not only on the surface of the each layer but also between the top and bottom layers due to the

strong coupling effect [29, 30]. Based on these observations, the currents between two layers create strong circular dichroism response due to FTEM waves [31, 32].

## 4 Conclusion

The new approach of FTEM wave is introduced to realize the polarization conversion. In this communication, the novel approach of FTEM waves is firstly introduced to achieve giant CD effect due to strong coupling of the electric and magnetic field. The perfect circular polarization and high efficiency of proposed structure are computed with HFSS simulation and validate its results by experimental. The designed structure possesses the high transmission efficiency at operated frequency bands. The simulated and measured results exhibit good correspondence. In addition, the proposed structure with high bandwidth could be expected by changing geometry stability of implemented SRR. The presented design is feasible to be constructed to higher scale array in terahertz and even optical region. This designed structure has good performance which is useful for various applications such as, remote sensors, antenna applications, and may be recommended for optical applications.

## References

1. Montejo-Garai, J. R., & Zapata, J. (1999). Full-wave design of dual-band double-septum circular waveguide polarizers. *Microwave and Optical Technology Letters*, 20(2), 99–103.
2. Mutlu, M., Akosman, A. E., & Ozbay, E. (2012). Broadband circular polarizer based on high-contrast gratings. *Optics Letters*, 37(11), 2094–2096.
3. Mutlu, M., Akosman, A. E., Kurt, G., Gokkavas, M., & Ozbay, E. (2012). Experimental realization of a high-contrast grating based broadband quarter-wave plate. *Optics Express*, 20(25), 27966–27973.
4. Mutlu, M., Akosman, A. E., Serebryannikov, A. E., & Ozbay, E. (2011). Asymmetric chiral metamaterial circular polarizer based on four U-shaped split ring resonators. *Optics Letters*, 36(9), 1653–1655.
5. Silveirinha, M. G. (2008). Design of linear-to-circular polarization transformers made of long densely packed metallic helices. *IEEE Transactions on Antennas and Propagation*, 56(2), 390–401.
6. Shatrow, A. D., Chuprin, A. D., & Sivov, A. N. (1995). Constructing the phase converters consisting of arbitrary number of translucent surfaces. *IEEE Transactions on Antennas and Propagation*, 43(1), 109–113.
7. Dietlein, C., Luukanen, A., Popovi, Z., & Grossman, E. (2007). A W-band polarization converter and isolator. *Transactions on Antennas and Propagation*, 55(6), 1804–1809.
8. Leong, K. M. K. H., & Shiroma, W. A. (2002). Waffle-grid polariser. *Electronics Letters*, 38(22), 1360–1361.
9. Mailloux, R. J. (2005). *Phased array antenna handbook*. Boston: Artech House.
10. Fartookzadeh, M., & MohseniArmaki, S. H. (2016). Enhancement of dual-band reflection-mode circular polarizers using dual-layer rectangular frequency selective surfaces. *IEEE Transactions on Antennas and Propagation*, 64(10), 4570–4574.
11. Cao, H., Liang, J., Wu, X., et al. (2016). Dual-band polarization conversion based on non-twisted Q-shaped metasurface. *Optics Communications*, 370, 311–318.
12. Silveirinha, M. G. (2008). Design of linear-to-circular polarization transformers made of long densely packed metallic helices. *IEEE Transactions on Antennas and Propagation*, 56(2), 390–401.
13. Mutlu, M., Akosman, A. E., Serebryannikov, A. E., & Ozbay, E. (2011). Asymmetric chiral metamaterial circular polarizer based on four U-shaped split ring resonators. *Optical Letter*, 36(9), 1653–1655.
14. Cheng, Y., Nie, Y., Cheng, Z., & Gong, R. Z. (2014). Dual-band circular polarizer and linear polarization transformer based on twisted split-ring structure asymmetric chiral metamaterial. *Progress in Electromagnetics Research*, 145, 263–272.
15. Fonseca, N. J. G., & Mangenot, C. (2016). High-performance electrically thin dual-band polarizing reflective surface for broadband satellite applications. *IEEE Transactions on Antennas and Propagation*, 64(2), 640–649.

16. Mangi, F. A., Xiao, S., Mallah, G. A., et al. (2017). Multi-band circular polarizer based on periodic metallic strip array. *International Journal of Engineering Systems Modelling and Simulation*, 9(3), 143–149.
17. Cao, T., & Cryan, M. J. (2012). Enhancement of circular dichroism by a planar non-chiral magnetic metamaterial. *Journal of Optics*, 14(8), 085101. <http://dx.doi.org/10.1364/OE.16.011802>
18. Doumanis, E., Goussetis, G., Gomez-Tornero, J. L., et al. (2012). Anisotropic impedance surfaces for linear to circular polarization conversion. *IEEE Transactions on Antennas and Propagation*, 60(1), 212–219.
19. Lin, X. Q., & Cui, T. J. (2008). Controlling the bandwidth of split ring resonators. *IEEE Microwave and Wireless Components Letters*, 18(4), 245–247.
20. Zhu, X.-C., Hong, W., Wu, K., et al. (2014). Design of a bandwidth-enhanced polarization rotating frequency selective surface. *IEEE Transactions on Antennas and Propagation*, 62(2), 940–944.
21. Chen, J., & Zhang, A. (2013). A linear-to-circular polarizer using split ring resonators. *Applied Computational Electromagnetics Society Journal*, 28(6), 507–512.
22. Chen, H., Ma, H., Wang, J., et al. (2016). Ultra-wideband transparent 90° polarization conversion metasurfaces. *Applied Physics A*, 122(46), 2–5.
23. Zarifi, D., Soleimani, M., & Nayyeri, V. (2012). Dual-and multiband chiral metamaterial structures with strong optical activity and negative refraction index. *IEEE Transactions Wireless Propagation Letter*, 11, 334–337.
24. Volski, V., Vandenbosch, G. A. E., & Vasylychenko, A. (2011). A dedicated technique to measure shielding effectiveness of textiles using a two horn-antenna set-up. *The Journal of The Textile Institute*, 102(2), 164–171.
25. Singh, R., Ai-Naib, I. A. I., Koch, M., & Zhang, W. L. (2011). Sharp Fano resonances in THz metamaterials. *Optical Express*, 19, 6312–6319.
26. Shi, J. H., Zhu, Z., Ma, H. F., Jiang, W. X., & Cui, T. J. (2012). Tunable symmetric and asymmetric resonances in an asymmetrical split-ring metamaterial. *Journal of Applied Physics*, 112(7), 073522. <https://doi.org/10.1063/1.4757961>
27. Ye, Y., & He, S. (2010). 90° polarization rotator using a bilayered chiral metamaterial with giant optical activity. *Applied Physics Letters*, 96(20), 203501. <https://doi.org/10.1063/1.3429683>
28. Huang, C., Ma, X., Pu, M., Yi, G., Wang, Y., & Luo, X. (2013). Dual-band 90° polarization rotoar using twisted split ring resonators array. *Optics Communications*, 291, 345–348.
29. Mangi, F. A., Xiao, S., Memon, I., & Jamro, D. A. (2016). Novel design and performance analysis of broadband dual layer circular polarizer based on frequency selective surface for 60 GHZ application. In: Zeng Q. A. (Ed.), *Wireless communications, networking and applications. Lecture notes in electrical engineering* (vol. 348, pp. 319–325). New Delhi: Springer.
30. Huang, C., Ma, X., Pu, M., Yi, G., Wang, Y., & Luo, X. (2013). Dual-band 90° polarization rotoar using twisted split ring resonators array. *Optics Communications*, 291, 345–348.
31. Mangi, F. A., Xiao, S., Mallah, G. A., et al. (2016). Multi-band circular polarizer based on fission transmission of linearly polarized wave for x-band applications. *Journal of Electrical and Computer Engineering*, 14, 8.
32. Mangi, F. A., Xiao, S., Yao, Z., et al. (2017). Double-layer broadband circular polarizer based on fission transmission of linear polarization for Ku-band applications. *Microwave and Optical Technology Letters*, 59, 2680–2685.



**Farman Ali Mangi** received Ph.D. in the field of electronics science and technology from University of Electronics Science and Technology, Chengdu, Sichuan, China. His research interests included Electronics, Antenna and Propagation, LASER Atomic Spectroscopy and Material Physics. Currently, he is working as Professor in the department of Physics and Electronics, Shah Abdul Latif University, Khairpur, Sindh, Pakistan. He received China Scholarship Council (CSC) excellent international student research award for the academic year 2015/2016 on dated 30 December 2015. He presented enough research papers in international conferences organized at Beijing, Shanghai, Shenzhen, Chengdu, Bangkok and Phuket. His research work is available on web of science, EI-Village, IEEE Explorer and published in reputed international journals of EI-Index and SCI (Springer and Elsevier) as well. He has authored/co-authored more than 50 technical journals and conference paper.



**Shaoqiu Xiao (M'05)** received Ph.D. degree in Electromagnetic field and Microwave Engineering from the University of Electronic Science and Technology of China (UESTC), Chengdu, China, in 2003. From January 2004 to June 2004, he joined UESTC as an assistant professor. From July 2004 to March 2006, he worked for the Wireless Communications Laboratory, National Institute of Information and Communications Technology of Japan (NICT), Singapore, as a researcher with the focus on the planar antenna and smart antenna design and optimization. From July 2006 to June 2010, he worked for UESTC as an associate professor and now he is working for UESTC as a professor. His current research interests include planar antenna and phased array, microwave passive circuits and time reversal electromagnetics. He has authored/coauthored more than 160 technical journals, conference papers, books and book chapters.

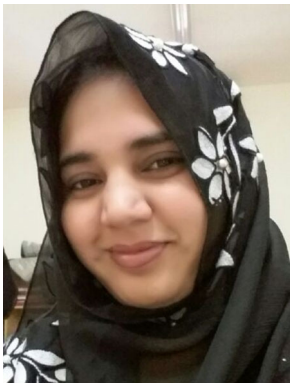


**Qasim Ali Arain** is a Ph.D. candidate at School of Electronic Engineering, Beijing University of Posts and Telecommunication, China. He is currently working as an Assistant Professor in Department of Software Engineering Mehran University of Engineering and Technology, Jamshoro, Pakistan. He has completed his Bachelors in Software Engineering from Mehran UET Jamshoro in 2005 and completed his Masters in Information Technology in 2010. He is a Cisco Certified Academy Instructor (CCAI), Cisco Security Specialist Microsoft Certified System Engineer (MCSE), Sun Certified Java Programmer SCJP. His current research interest includes Location based services, Network Security and Indoor positioning.



**Imran Memon** B.S. Electronics 2008 from ICT University of Sindh Jamshoro, Sindh Pakistan. M.E. Computer Engineering from University of Electronic Science and Technology, Chengdu Sichuan China. He is towards Ph.D. from College of Computer Science and Technology, Zhejiang University. He serves Editor-in-Chief Journal of Network Computing and Applications. He serves Editor of JDCTA, open computer science journal and Journal of Web Systems and Applications. He got Academic Achievement Award 2011–2012 from UESTC China and also got Excellent Performance Award 2011–2012 from UESTC China. He published over 30 research papers in recent years. He serves as an organizing committee chair and TPC member more than 250 international conferences, as well as a reviewer for over 50 international research journals, including IEEE Transactions on Circuits and Systems for Video Technology, IEEE Transactions on Image Processing, IEEE Transactions on Signal Processing, IEEE Transactions on Multimedia, IEEE Multimedia, IEEE Transactions on

Industrial Electronics, IEEE Signal Processing Letters, Journal of Electronic Imaging Information Sciences Computer Vision and Image Understanding, Image and Vision Computing, EURASIP Journal on Advances in Signal Processing, Computer Standards and Interfaces, Circuits Systems and Signal Processing Journal of Information Science and Engineering, International Journal of Computers and Applications Far East Journal of Experimental and Theoretical Artificial Intelligence, IEE Proceedings Vision, Image and Signal Processing, EURASIP Signal Processing IEE Proceedings Information Security, Journal of Circuit, System, and Signal Processing, International Journal of Computers and Applications, LNCS Transactions on Data Hiding and Multimedia Security, Signal Processing International Journal of Pattern Recognition and Artificial Intelligence, IEEE Transactions on Information Forensics and Security, IEEE Transactions on Vehicular Technology, Transactions on Internet and Information Systems, Wireless Personal Communication, Computers and Electrical Engineering, Computer Networks, Wireless Networks, IEEE Access, Telecommunication Systems and Others. Current research interests; Artificial Intelligence System, Network Security, Embedded System, Information Security, Peer to Peer Networks, Location Based Services, Road Network.



**Miss Ghulam Fatima Kakepoto** received B.S. degree in Physics. Currently, she is pursuing MS in Radio Physics, University of Electronic Science and Technology, Chengdu, Sichuan, China. Her research interests included Electronics, Antenna and Propagation. She worked as Lecturer in the department of Physics at University of Agriculture and Engineering, Khairpur, Sindh, Pakistan.